Inverse analysis of an embankment on soft clay using the Ensemble Kalman Filter

A. Hommels[(1)], F. Molenkamp[(1)], B. Nguyen[(3)], A.W. Heemink[(2)]

Faculty of Civil Engineering and Geosciences, Section of GeoEngineering[(1)]
Faculty of Electrical Engineering, Mathematics and Computer Science,
Department of Applied Mathematical Analysis[(2)],
TUDelft, Netherlands
Netherlands Organisation for Applied Scientific Research TNO,
Netherlands Institute of Applied Geoscience NITG[(3)],
Utrecht, Netherlands

Abstract

Geomechanical models are indispensable for reliable design of engineering structures and processes and hazard and risk evaluation. These models are however far from perfect. Errors are introduced by fluctuations in the input or by poorly known parameters in the model. To overcome these problems an inverse modelling technique to incorporate measurements into the deterministic model to improve the model results can be implemented. This allows for observations of on-going processes to be used for enhancing the quality of subsequent model predictions.
In geomechanics several examples of inverse modelling exist where the improved model of the system is obtained by minimizing the discrepancy between the observed values in the system and the modelled state of the system within a time interval. This requires the implementation of the adjoint model. Even with the use of the adjoint compilers that have become available recently, this is a tremendous programming effort for the existing geomechanical model system.
Therefore, the Ensemble Kalman filter is implemented to overcome this problem. The Ensemble Kalman filter is already rather common in meteorology and oceanography and the state of the system is analysed each time data becomes available. An additional challenge is the influence of the heterogeneity of the ground.
Very promising results of a conceptual example, based on the construction of a road embankment on soft clay, are presented. The Ensemble Kalman filter is not only used for a straight forward identification of the elastic modulus E and the K_0 parameter of several soil layers below the embankment, but also incorporates the uncertainty of the exact location of the boundaries between the subsequent layers.

Keywords: Inverse modelling, soil properties, Ensemble Kalman filter

1 Introduction

In geotechnical engineering context inverse modelling or back analysis consists in finding the values of the mechanical parameters, or of other quantities characterizing a soil or rock mass, that when introduced in the stress analysis of the problem under examination lead to results (e.g. displacements, stresses etc.) as close as possible to the corresponding in situ measurements. Already in the 1980s the use of data from in situ measurements as input for inverse modelling was proposed by Gioda et al. [5,6] and Cividini et al. [1,2]. By then inverse modelling was mostly referred to as back analysis or parameter estimation. The optimal state of the system is obtained by minimizing the discrepancy between the observed values in the system and the forecasted state of the system within a time interval. The method can be subdivided into least-squares method, Maximum Likelihood and (Extended) Bayesian Method, based on their capability to cope with different types of prior information. In the nineties several articles are published bases on this type of inverse modelling [4,7,8]. However recent developments in other fields of science have shown a new powerful technique indicated as the Ensemble Kalman filter. In a filter, the state of the system is analysed each time data becomes available. The total computational effort compared to the above-mentioned methods is the same, but a filter is easier to implement.
The general formulations of this filter as well as a case study will be discussed in the next sections.

All measurements in this case study are created in order to check the performance of the Ensemble Kalman filter first and due to the lack of “real” data of simple case studies.
The values for the properties of the soil layers below the embankment are derived from the embankment as described in Honjo et al. [7,8]. Indraratna et al. [9] describe the same embankment, including several field measurements and laboratory test results, which makes my case study more realistic.

2 Theory

2.1 Basic concepts and definitions

Let the state vector $x^t(k)$ describe the state at a time step k of a physical system, such as the subsurface. The elements of the state vector are filled with stresses but possibly also strains or other state parameters. The superscript 't' denotes that $x^t(k)$ is the "true" state; the exact value is probably unknown. To obtain insight in the true state, a model is developed to make a forecast $x^f(k+1)$ at time step $k+1$:

$$x^f(k+1) = M(x^f(k)) \tag{1.1}$$

The superscript 'f' denotes that $x^f(k)$ is a "forecast" of the true state $x^t(k)$ at time step k, in the best case a good approximation. In the context of the shallow subsurface, the state vector can be filled partly with displacements u. M denotes the dynamical model operator, which describes for instance the constitutive model of the soil, e.g. the soil parameters E and ν in the simplest elastic case. If there are uncertainties in

the parameters, which have to be updated, the state vector $x^f k)$ is also filled with the uncertain parameters.

Since models are never perfect:

$$x^t(k) = x^f(k) + \eta(k) \qquad (1.2)$$

in which $\eta(k)$ is the unknown model error in the *k-th* forecast with $E\{\eta\}=0$ and $E\{\eta^2\}= P$ (E denotes expection), which is the model error covariance matrix.
Some entities of the state are compared with data from an observational network, for example the measurements y^o of the surface displacements. All available data for time step k are stored in an observation vector $y^o(k)$. The superscript 'o' denotes that $y^o(k)$ is an "observation". There is a difference $\varepsilon(k)$ between the "true" state $x^t(k)$ and the actual "observed" data $y^o(k)$:

$$y^o(k) = H(k)x^t(k) + \varepsilon(k) \qquad (1.3)$$

where $H(k)$ is the linear observational operator. The observations are assumed unbiased $(E\{\varepsilon\}=0)$ and $E(\varepsilon^2)= R$), which is the measurement error covariance matrix.
In general some background information $x^p(k=0)$ is available from e.g. site investigation, where the time $t=0$ is the start of the observation for the current project, indicated by time step $k=0$. The superscript $'p'$ denotes that $x^p(k=0)$ contains "prior" information of the unknown parameters to be estimated, which are collected in model parameter vector θ. At the start of the construction, time step k=0, $E\{x^p\}= E\{\theta\}$. During the construction, for each timestep k, there will be an increasing difference $\delta(k)$ between $x^p(k)$ and $\theta(k)$:

$$\theta(k) = x^p(k) + \delta(k) \qquad (1.4)$$

The prior error covariance matrix S is defined as $S =\mathrm{E}\{(\theta - x^p)^T(\theta - x^p)\}$.
All the different terms for the minimization process refer to the fact that these methods try to merge prior information, model forecasts and measurements using the benefits of every source of information, namely x^p, x^t and y^O. These sources are merged to create a new "analysed" state x^a; x^a is the "analysed" model forecast using the measurements y^o and prior information x^p.
The final goal of inverse modelling methods is to improve the state vector; at each time step k measurements become available, with an error (k) as small as possible. For this minimization process several names exists: inverse analysis, back analysis, parameter estimation procedure and data assimilation (meteorology).

2.2 Kalman filters

In a filter, the state of the system is analysed each time data becomes available. In variational methods, all data of each time step in the interval is used. The total computational effort for each method is the same, however, a filter is easier to implement than a variational method.
In 1960, R.E. Kalman [11] published his famous paper in which he describes a recursive solution to the discrete data linear filtering problem. Murakami [13] performed his Ph.D. on the application of the linear Kalman filter on geomechanical problems and published several articles [14,15] on the use of the linear Kalman filter

for geomechanical applications. In the field of meteorology also several examples exist for the application of the Extended and the Ensemble Kalman filters.
The algorithms of the Kalman filters are briefly reviewed in the coming sections. Details of these are given in Jazwinsky [] and Evensen [].

2.2.1 Linear Kalman filter

A discrete model for the evolution of a physical process from time step k to time step $k+1$ is governed by the linear stochastic equation:

$$x^f(k+1) = A(k)x^t(k) + B(k)u(k) + G(k)w(k) \quad (1.5)$$

in which A(k) represents the linear system operator and relates the true state x^t at time step k to the forecasted state x^f at time step $k+1$,$B(k)$ is an input matrix, $u(k)$ is the system input, $G(k)$ is the noise input matrix and $w(k)$ is the process noise with zero mean and covariance matrix Q.
In the time update step, the modelled state vector is calculated based on the analysed state of the previous time step:

$$x^f(k+1) = A(k)x^a(k) + B(k)u(k) \quad (1.6)$$

$$P^f(k+1) = A(k)P^a(k)A^T(k) + G(k)Q(k)G^T(k) \quad (1.7)$$

where P^f is the forecasted error covariance matrix. Then in the measurement update step, the forecasted statevector $x^f(k+1)$ is weighted to the observational vector $y^o(k+1)$ by means of the Kalman gain K to give the analysed estimate $x^a(k+1)$:

$$x^a(k+1) = x^f(k+1) + K(k+1)\left\{y^o(k+1) - H(k+1)x^f(k+1)\right\} \quad (1.8)$$

$$P^a(k+1) = \left\{I - K(k+1)H(k+1)\right\}P^f(k+1) \quad (1.9)$$

where P^a is the analysed error covariance matrix. The Kalman gain $K(k+1)$ is defined as:

$$K(k+1) = \frac{P^f(k+1)H^T(k+1)}{H(k+1)P^f(k+1)H^T(k+1) + R(k+1)} \quad (1.10)$$

2.2.2 Extended Kalman filter (EKF)

The linear Kalman filter is designed for linear systems. It is, however, possible to derive approximate filters using linearization techniques for non-linear systems. Assume that the system again can be described by a state vector x, but that the physical process is now governed by the non-linear stochastic equation:

$$x^f(k+1) = f(x^t(k), u(k)) + G(k)w(k) \quad (1.11)$$

In the time update step, the equations can now be written as:

$$x^f(k+1) = f(x^a(k), u(k)) \quad (1.12)$$

$$P^f(k+1) = F(k)P^a(k)F^T(k) + G(k)Q(k)G^T(k) \quad (1.13)$$

where

$$F(k) = \left(\frac{\partial f}{\partial x}\right)_{x_{ref}} \quad (1.14)$$

The measurement update equations can be written as follows:

$$x^a(k+1) = x^f(k+1) + K(k+1)\left\{y^o(k+1) - H(k+1)x^f(k+1)\right\} \quad (1.15)$$

$$P^a(k+1) = \left\{I - K(k+1)H(k+1)\right\} P^f(k+1) \quad (1.16)$$

and the Kalman gain remains the same as equation (1.10).

2.2.3 Ensemble Kalman filter (EnKF)

Evensen introduced the Ensemble Kalman filter in 1994 (Evensen, 1994) and the theoretical formulations as well as an overview of several applications are described in Evensen (2003). The EnKF was designed to resolve two major problems related to the use of the extended Kalman filter. The first problem relates to the use of an approximate closure scheme in the EKF, and the other one to the huge computational requirements associated with the storage and forward integration of the error covariance matrix P^a. For further details the reader is referred to the references.

In the Ensemble Kalman filter, an ensemble of possible state vectors, which are randomly generated using a Monte Carlo approach, represents the statistical properties of the state vector. The algorithm does not require a tangent linear model, which is required for the EKF, and is very easy to implement.

At initialisation, an ensemble of N initial states $(\xi_N)_0$ are generated to represent the uncertainty at time step $k=0$. In the measurement update step, the matrix $E^f(k+1)$ defines an approximation of the covariance matrix $P^a(k+1)$ (equation (1.19) and equation (1.20)).

The time update equations for the Ensemble Kalman filter for each estimate of the state are:

$$\xi_i^f(k+1) = f(\xi_i^a(k)) + G(k)w(k) \quad (1.17)$$

$$x^f(k+1) = \frac{1}{N}\sum_{1}^{N}\xi_i^f(k+1) \quad (1.18)$$

$$E^f(k+1) = [\xi_1^f(k+1) - x^f(k+1),\ldots,\xi_N^f(k+1) - x^f(k+1)] \quad (1.19)$$

In the measurement update step:

$$P^a(k+1) = \frac{1}{N-1}E^f(k+1) * (E^f(k+1))^T \quad (1.20)$$

Equation (1.20) is never really calculated due to huge computational requirements, as mentioned before, but is split up:

$$K(k+1) = \frac{E^f * ((E^f)^T * H)}{N-1}\left[H\frac{1}{N-1}E^f * ((E^f)^T * H^T) + R\right]^{-1} \quad (1.21)$$

$$\xi_i^a(k+1) = \xi_i^f(k+1) + K\left\{y_o(k+1) - H\xi_i^f(k+1) + \varepsilon\right\} \quad (1.22)$$

where ε is for each ensemble member a randomly added measurement error (Evensen, 2003).

3. Casestudy

3.1 Description of the case

For this study, a 4-meter high embankment constructed on soft clay has been considered.

3.1.1 Finite element modelling

A dedicated model for determination of the settlement has been written using Griffith and Smith []. In ***figure 1*** the finite element mesh is shown, which consists of 294 nodes and 98 elements.

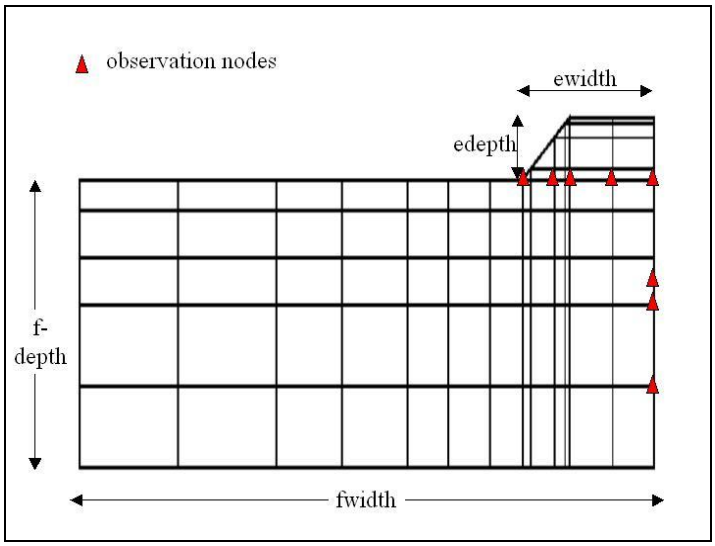

figure 1: finite element mesh for embankment

The nodes at which the observations of the vertical displacement took place are indicated with a red triangle.

The embankment is built in four lifts and at the end of each lift a consolidation period is considered. In figure 2 the different stages and their total time are shown.

3.1.2 Material properties

Two different models are used to identify the uncertain parameters. The Young's modulus E and the horizontal permeability k_h are the uncertain parameters of the layer(s) beneath the embankment Honjo et al. []). These parameters have to be estimated during the construction process.
Model 1 consists of one layer as foundation. Throughout this layer the soil properties are kept constant. A schematic overview is shown in figure 3.
The properties of the soil layer and the embankment of model 1 are listed in table 1.

Soil layer	E(kPa)	ν	c	φ	ψ	γ(kN/m^3)	k_h(m/day)	k_v(m/day)
1	*3400*	*0.33*	*14.0*	*20.0*	*0*	*16.0*	*0.00009*	*0.000005*
embankment	*5100*	*0.3*	*19*	*26*	*0*	*20.5*	-	-

table 1: material properties 1-layered foundation

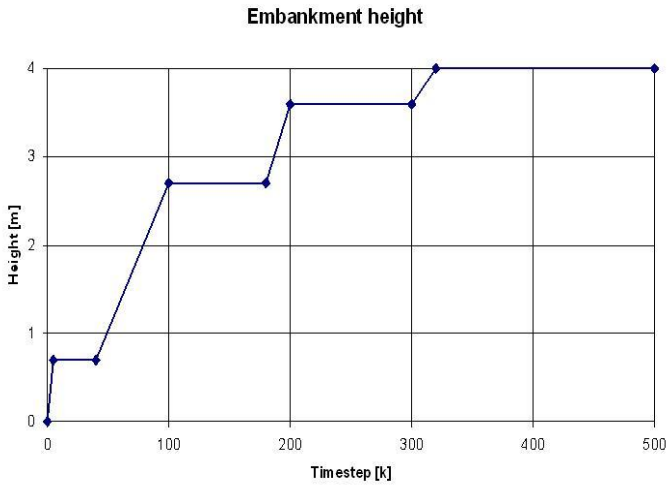

figure 2: embankment height during the construction phases

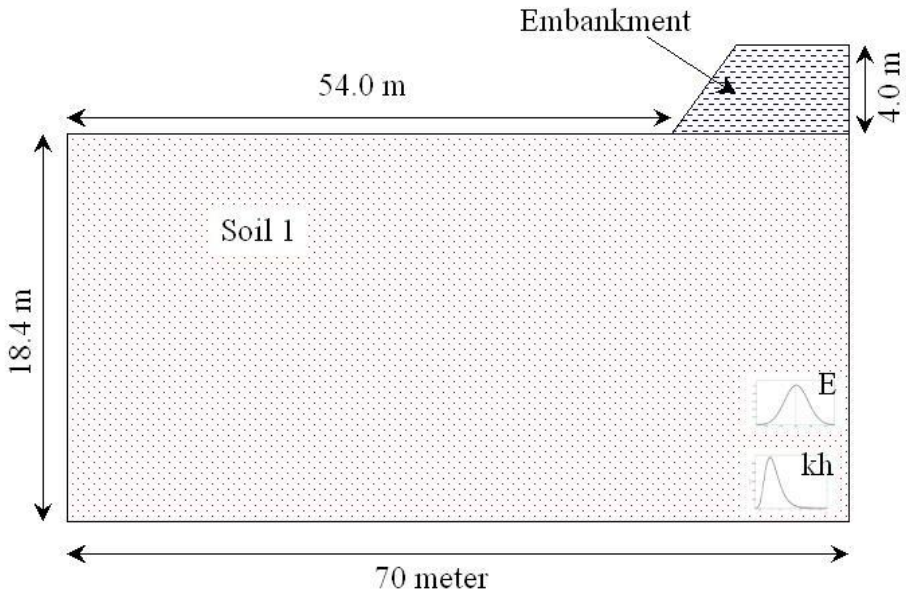

figure 3: 1-layered foundation

The Young's modulus E has a normal distribution, with mean $\mu = 3400\ kPa$ and standard deviation $\sigma = 150\ kPa$ at time step $k=0$. The horizontal permeability k_h has a lognormal distribution with mean $log(\mu) = -11.6183\ log\ (m/day)$ and standard deviation $\sigma = 0.33\ log\ (m/day)$ at k=0.

Model 2 (figure 4) consists of three different soil layers in the foundation. This model is fully based on the description of the embankment as described in Honjo et al. (1994a,b) and Indraratna et al. (1992). The properties of the subsequent layers in

the foundation as well as the embankment fill are based on the values as described in these articles.

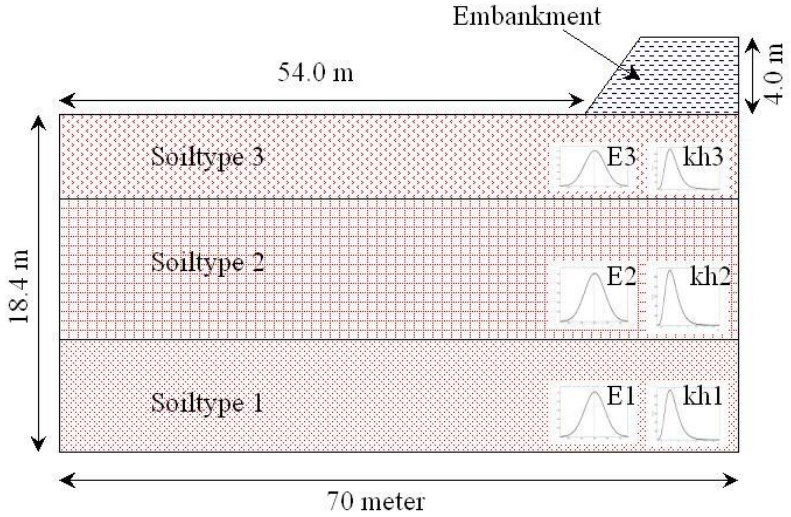

figure 4: 3-layered foundation

The properties of the soil layers and the embankment are listed in table 2.

Soil layer	E(kPa)	ν	c	φ	ψ	γ(kN/m^3)	k_h(m/day)	k_v(m/day)
1	*3400*	*0.33333*	*16*	*12.5*	*0*	*16.5*	*2.41E-05*	*2.94E-05*
2	*1400*	*0.33333*	*22*	*13.5*	*0*	*15.6*	*8.34E-05*	*8.99E-05*
3	*4600*	*0.3*	*8*	*6.5*	*0*	*17.3*	*3.56E-04*	*1.03E-04*
embankment	*5100*	*0.3*	*19*	*26*	*0*	*20.5*	-	-

table 2: material properties 3-layered foundation

The Young's *E* moduli have a normal distribution, with mean μ_1 *=3400 kPa*, μ_2 *=1400 kPa* and μ_3 *=4600 kPa*; the standard deviation σ_i*=0.1* μ_i kPa* for *i=1,2,3* at time step k=0. The horizontal permeability k_h has a lognormal distribution with mean *log(μ_1)=-10.6333 log (m/day)*, mean *log(μ_2)=-9.3919 log (m/day)* and *mean log(μ_3)=-7.9406 log (m/day)*; standard deviation σ_i*=0.33 log (m/day)* for *i=1,2,3* at time step k=0.

3.1.3 Measurements

The measurements for model 1 are created using the material properties as listed in table 3.

Soil layer	E(kPa)	ν	c	φ	ψ	γ(kN/m^3)	k_h(m/day)	k_v(m/day)
1	*3900*	*0.33*	*14.0*	*20.0*	*0*	*16.0*	*0.00011*	*0.000005*
embankment	*5100*	*0.3*	*19*	*26*	*0*	*20.5*	-	-

table 3: material properties measurements 1-layered foundation

The measurements for model 2 are created using the material properties as listed in table 4.

Soil type	E(kPa)	ν	c	φ	ψ	γ(kN/m^3)	k_h(m/day)	k_v(m/day)
1	*3900*	*0.33333*	*16*	*12.5*	*0*	*16.5*	*4.41E-05*	*2.94E-05*
2	*1800*	*0.33333*	*22*	*13.5*	*0*	*15.6*	*1.34E-04*	*8.99E-05*
3	*4800*	*0.3*	*8*	*6.5*	*0*	*17.3*	*1.56E-04*	*1.03E-04*
embankment	*5100*	*0.3*	*19*	*26*	*0*	*20.5*	-	-

table 4: material properties measurements 3-layered foundation

3.2 Results

In order to check the performance of the filter, first there was no noise added to the measurements.

3.2.1 No measurement noise

In figure 5 and figure 6 the update processes of Young's modulus *E* and horizontal permeability k_h through time for the 1-layered foundation are shown.

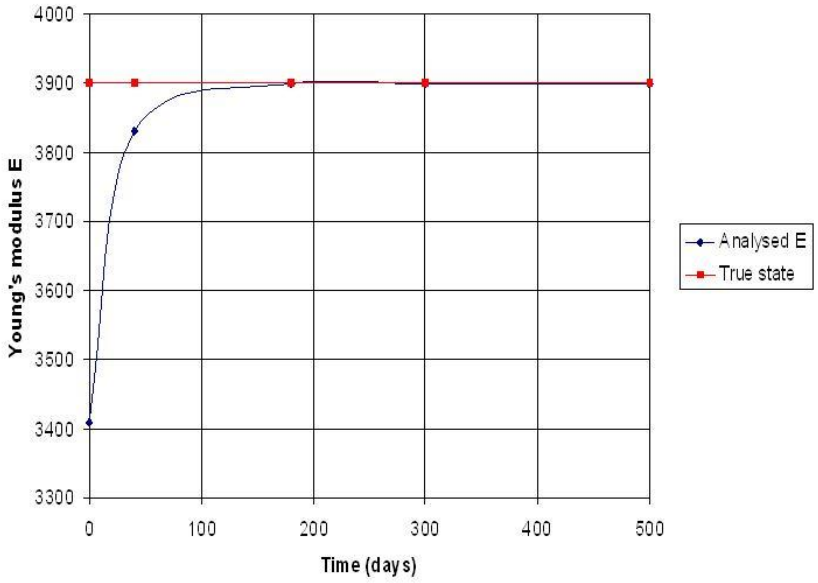

figure 5: update Young's modulus E for the one-layered distribution

The update of the Young's modulus *E* is going very fast: within two analyses the true state is reached as can be seen in figure 5. Also the update of the horizontal permeability k_h goes fast: within three analyses the true state is reached (figure 6).
Since the measurements are indicated as being perfect, the filter is completely relying on the measurements and gives the measurements a high weight compared to the modelled values. The properties of the distributions of the analysed uncertain parameters at the end of each lift are shown in table 5. These numbers confirm the confidence of the filter that measurements are perfect.

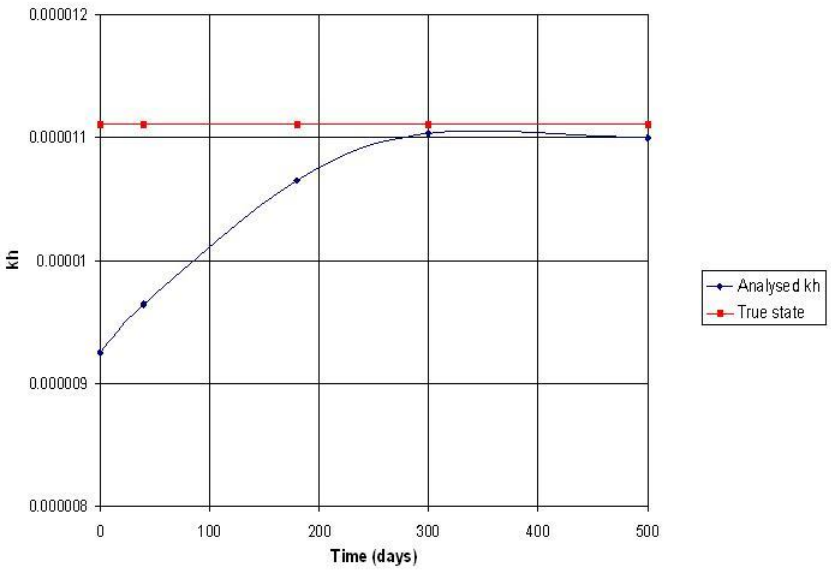

figure 6: update horizontal permeability k_h

Lift		mean μ_E	sd σ_E		logmean μ_{kh}	sd σ_{kh}
0		*3408.23*	*150.072*		*-11.5916*	*0.31532*
1		*3830.51*	*13.361*		*-11.5497*	*0.314985*
2		*3899.32*	*0.230476*		*-11.4505*	*0.0583542*
3		*3899.33*	*0.05797*		*-11.4153*	*0.00264911*
4		*3899.32*	*0.057833*		*-11.4181*	*0.00229442*

table 5: properties of the distributions at the end of each lift

For the 3-layered foundation the update processes for the Young's moduli E and horizontal permeabilities k_h through time are shown in figure 7 and figure 8. The update of the Young's modulus E is going very fast: again, as in the one-layered foundation the true state is reached within two analyses. The update of the horizontal permeability k_h goes also fast for soil layer 1 and 2: within three analyses the true state is reached. However, the true state of the horizontal permeability k_h of soil layer 3 converges very slowly and doesn't reach the true state at all.
The properties of the distributions of the analysed uncertain parameters at the end of each lift are shown in table 6 and table 7.

Lift		mean $\mu_{E,1}$	sd $\sigma_{E,1}$	mean $\mu_{E,2}$	sd $\sigma_{E,2}$	mean $\mu_{E,3}$	sd $\sigma_{E,3}$
0		*3413.5*	*208.2*	*1405.09*	*333.392*	*4593.44*	*195.922*
1		*3885.6*	*16.132*	*1666.2*	*55.1307*	*4678.09*	*66.0857*
2		*3873.86*	*11.1163*	*1772.16*	*12.6084*	*4783.15*	*19.5107*
3		*3874.55*	*10.2213*	*1790.58*	*7.72335*	*4791.73*	*7.49312*
4		*3884.37*	*7.29639*	*1787.66*	*4.06907*	*4787.09*	*4.53743*

table 6: properties of the distribution of the Young's moduli E

Lift		logmean $\mu_{kh,1}$	sd $\sigma_{kh,1}$	logmean $\mu_{kh,2}$	sd $\sigma_{kh,2}$	logmean $\mu_{kh,3}$	sd $\sigma_{kh,3}$
0		*-10.6489*	*0.316352*	*-9.39773*	*0.346859*	*-7.87306*	*0.347388*
1		*-10.6451*	*0.306411*	*-9.06438*	*0.248114*	*-7.87306*	*0.339702*
2		*-10.4647*	*0.213307*	*-9.07174*	*0.060108*	*-8.24917*	*0.322095*
3		*-10.0754*	*0.057803*	*-8.99694*	*0.042527*	*-8.34798*	*0.268733*
4		*-10.1219*	*0.04512*	*-9.01219*	*0.033237*	*-8.36236*	*0.267652*

table 7: properties of the log(horizontal permeabilities)

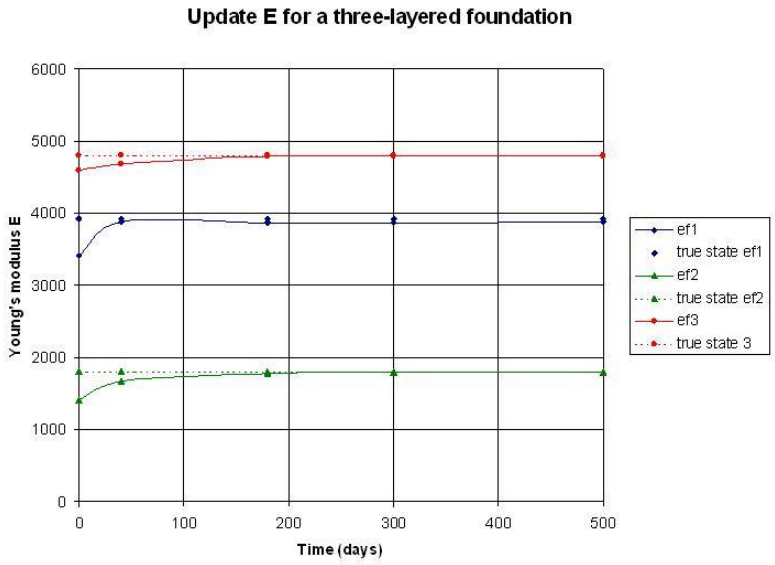

figure 7: update Young's moduli E for the 3-layered distribution

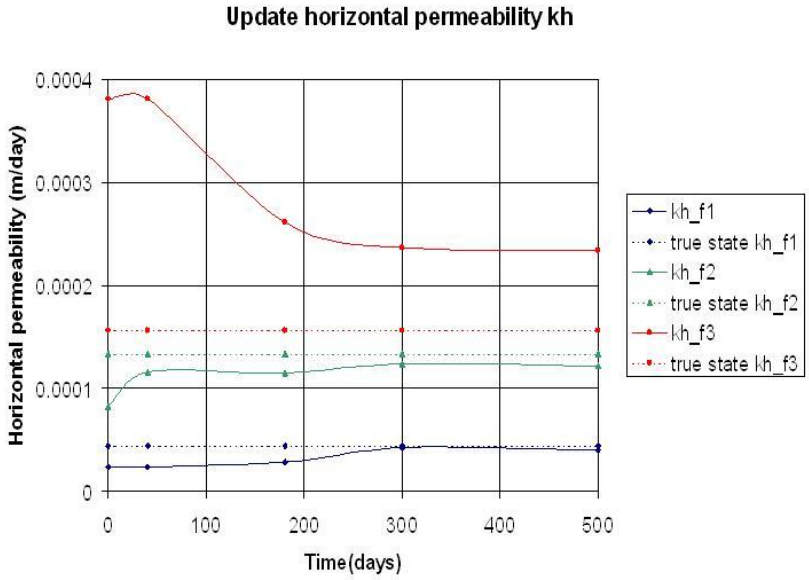

figure 8: update horizontal permeability k_h for the 3-layered distribution

3.2.1 Measurement noise

Since in real life, measurements are never performed perfectly, some noise is added to the measurements. The noise is normally distributed with mean $\mu = 0$, standard distribution $\sigma = 0.1$ and constant through time (i.e. white noise).

First the measurement noise is added to the model with only 1 layer in the foundation. The results for the update processes of Young's modulus E and horizontal permeability k_h through time are shown in

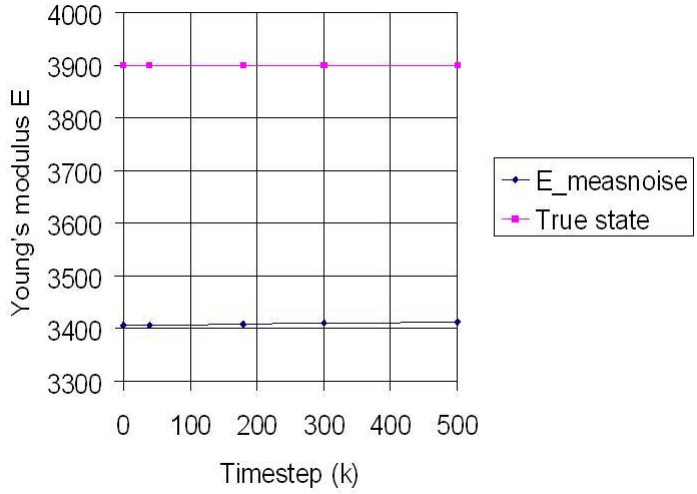

figure 9: update Young's modulus E including measurement noise

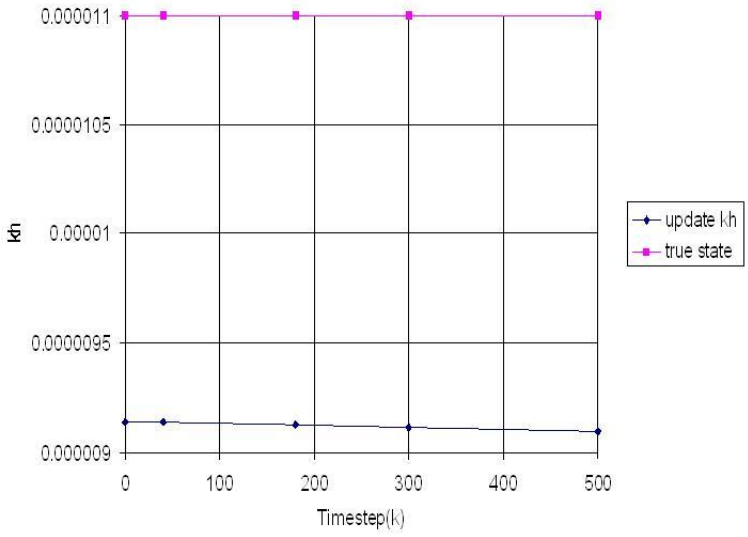

figure 10: update horizontal permeability k_h including measurement noise

In table 8 the properties of the distributions of the uncertain parameters are shown. The distribution of Young's modulus E only changes slightly. It is clear from this

table that the mean μ of the Young's modulus E increases very slowly and the standard deviation σ is decreasing very slowly.
The properties of the distribution of the horizontal permeability k_h don't change at all. The filter interprets the measurements as very unreliable and updates the uncertain parameters very slowly.

Lift		mean μ_E	sd σ_E		logmean μ_{kh}	sd σ_{kh}
0		*3405.55*	*153.595*		*-11.603*	*0.290262*
1		*3405.57*	*154.105*		*-11.603*	*0.290299*
2		*3407.57*	*154.698*		*-11.604*	*0.290467*
3		*3410.55*	*153.578*		*-11.6055*	*0.290984*
4		*3413.46*	*151.083*		*-11.6075*	*0.291086*

table 8: properties distributions including measurement noise

Since the results for the 1-layered foundation including measurement noise in the analysis are very pour, the measurement noise is not added for the 3-layered foundation.

4. Conclusions and recommendations

4.1 Conclusions

In the case where no measurement noise is considered, for both the 1-layered as the 3-layered model, the true state for both the horizontal permeabilities k_h as well as the Young's moduli E is reached very fast. Very few analysis steps are necessary.
Only for soil layer 3, in the 3-layered model, the true state of the horizontal permeability k_h isn't reached at all. The filter doesn't rely on the measurements. This can be explained by the location of the observation nodes. In soil layer 3, the upper soil layer, these are located at the surface, where the water level equals zero and therefore also no water flow. The locations of the observation points are therefore very important.

However measurements are never perfect. That's why in the second case measurement noise is included. This is only carried out for model with 1 layer in the foundation, since the results showed that 4 analysis steps are by far not enough to reach the true state. In order to get a reasonable estimate of the uncertain parameters at least 500 analyses are necessary. Also the amount of information fed to the filter is very important.

4.2 Recommendations

Since the dedicated script is only feasible to perform a Kalman filter analysis at the end of each lift and the results for the case with no measurements are really promising, it is recommended to rewrite the script in such a way that an analysis can be performed after each time step. The authors are working on this at the moment.

5. Future developments

In the present case study only the measurement noise is incorporated. However several other types of uncertainties are present. One of the main features which is implemented at the moment is the localisation of uncertain boundaries between different soil layers using the Ensemble Kalman filter. Also the model noise has to be considered. During the presentation the results will probably be shown.

References

[1] Cividini, A. , L.Jurina and G.Gioda, *"Some aspects of 'characterization' problems in geomechanics"*. Int. Journal of Rock Mech. and Min. Science and Geom., vol. 18, 487-503 (1981).

[2] Cividini, A.., G.Maier and A.Nappi, *"Parameter estimation of a statistical geotechnical model using a Bayes' approach"*. Int. Journal of Rock Mech. And Min. Science, vol. 20, 215-226 (1983).

[3] Evensen, G., *"Sequential data assimilation with non-linear quasi-geostrophic model using Monte Carlo methods to forecast error statistics"*. Journal of Geoph. Research, vol. 99, C5/10, 143-162 (1994).

[4] Gens, A., Ledesma, A. and Alonso, E., "*Estimation of parameters in geotechnical backanalysis – II. Application to a tunnel excavation problem"*. Computers and Geotechnics, Vol. 18, No.1, p. 29-46 (1996).

[5] Gioda, G. and G. Maier, *"Direct search solution of an inverse problem in elastoplasticity: identification of cohesion, friction angle and in situ stress by pressure tunnel tests"*. Int. Journal for Num. and Anal. Methods in Geomechanics, vol. 4, 15, 1832-1848 (1980).

[6] Gioda, G., "*Some remarks on back analysis and characterization problems in geomechanics"*. Proc. 5th Int. Conf. On Numerical Methods in Geomechanics, Nagoya (1985).

[7] Smith, I.M. and D.V. Griffiths, Programming the finite elememt method. Chichester, Wiley and sons (2004).

[8] Honjo, Y., W.T. Liu and G. Soumitra , *"Inverse analysis of an embankment on soft clay by extended Bayesian method*". Int. Journal for Num. and Anal. Methods in Geomechanics, vol. 18, 709-734 (1994a).

[9] Honjo, Y., L. wen-Tsung, S. Sakajo , *"Application of Akaike information criterion statistics to geotechnical inverse analysis: the extended Bayesian method"*. Structural safety, vol. 14, 5-29 (1994b).

[10] Indraratna, B., A. S. Balasubramaniam and and S. Balachandran, "*Performance of test embankment constructed to failure on soft marine clay*". Journal ofGeotechnical engineering, vol. 118, 1, 12-33 (1992).

[11] Jazwinsky, A.H. , Stochastic processes and filtering theory, New York, Academic Press (1970).

[12] Kalman, R.E., *"A new approach to linear filter and prediction theory"*. Journal of Basic Engineering, 82D, 35-45 (1960).

[13] Ledesma, A., Gens and A., Alonso, E., "*Estimation of parameters in geotechnical back analysis – I. Maximum Likelihood Approach*". Computers and Geotechnics, Vol. 18, No.1, p. 1-27 (1996b).

[14] Murakami, A. , Studies on the application of Kalman filtering to some geotechnical problems related to safety assessment, Dissertation, Kyoto University (1991).
[15] Murakami, A. and T. Hasegawa, *"Application of Kalman filtering to inverse problems"*. Theor. and Appl. Mechanics, 42, 3-14 (1993).
[16] Murakami, A., *"Application of inverse analyses to Engineering problems"*. Theoretical and Applied mechanics, 46, 25-37 (1997).